Nuclear Inst. and Methods in Physics Research, A 899 (2018) 80–84

Contents lists available at ScienceDirect

Nuclear Inst. and Methods in Physics Research, A

journal homepage: www.elsevier.com/locate/nima

Measurement of neutrons down to 200 keV with pulse shape discrimination using an EJ-301 liquid scintillator

A.M. Lewis *, E. Blain, A.M. Daskalakis, Y. Danon

Gaertner LINAC Center, Rensselaer Polytechnic Institute, Troy, NY 12180, USA

ARTICLE INFO

Keywords:
Neutrons
PSD

ABSTRACT

Pulse shape discrimination is a method commonly used to separate gamma and neutron signals in liquid scintillation detectors. The method works well for neutrons above 500 keV, but as the energy deposited in the detector decreases, so does the effectiveness. In order to utilize pulse shape discrimination capabilities at lower energies, a 1.27 cm thick EJ-301 detector operated at a bias voltage of 2200 V has been used. The detector has been shown to have an average misclassification of 0.5% of gamma pulses over the total energy range from 35 keVee to 400 keVee, and 2.0% in the most sensitive region from 35 keVee to 45 keVee. A measurement performed using the time-of-flight method at the Gaertner Linear Accelerator Facility at Rensselaer Polytechnic Institute has shown that with the pulse shape discrimination method, this detector can detect and characterize neutron pulses down to 200 keV.

1. Introduction

Detection of keV-energy neutrons is important in the measurement of fission and neutron scattering data, nuclear nonproliferation and interrogation analysis of nuclear material. These measurements are often accompanied by a high gamma background, and a method of discrimination between the neutron and gamma interactions is necessary. At thermal and epithermal energies, detectors can take advantage of the large energy release of nuclear reactions such as the ^{10}B and ^{6}Li(n,α) reactions. However, these detectors suffer from low efficiency at higher energies. The neutron detection efficiency of a 9 mm thick Li glass detector peaks at 6% around 250 keV [1] which is the peak of the ^{6}Li resonance. Liquid scintillation detectors can have much greater efficiencies in the keV region and a similar sized EJ-301 detector has a neutron detection efficiency of approximately 53% at 250 keV. This increase in neutron detection efficiency makes EJ-301 a desirable detector in this energy range; however, liquid scintillators also have a high gamma detection efficiency and these gammas must be discriminated against in order to achieve a usable measurement. Pulse shape discrimination (PSD) techniques have been extensively developed and demonstrated for neutron energies above 500 keV [2], but difficulties exist in extending pulse shape discrimination below this threshold. As the neutron energy decreases, the probability of gamma rays being falsely classified as neutrons, which is referred to as the gamma misclassification rate, also increases.

A common method for testing PSD is to calculate a PSD parameter for each pulse based on the difference between the long and short charge integrations. A figure of merit is then calculated by dividing the separation between the gamma parameter distribution and the neutron parameter distribution by the widths of these distributions. Many PSD studies with EJ-301 detectors focus on this figure of merit and do not present results for pulse classification accuracy [3,4]. One study comparing four different PSD methods did present the rate of correct neutron pulse identification, but did not test their gamma misclassification rates [5]. However, similar work has been performed on EJ-309 detectors, using reference pulse shapes for energy deposition below 70 keVee [6]. That method was shown to classify neutrons down to 200 keV, and have a 5% misclassification rate of gammas between 35 and 45 keVee [6]. In this work we are focusing on reducing this misclassification rate using an EJ-301 detector and validating the minimal detectable neutron energy through time-of-flight measurements. This work attempts to improve keV-energy neutron detection by using a 1.27 cm thick EJ-301 detector operated at high bias voltage reduce this misclassification rate and validate the minimal detectable neutron energy through time-of-flight measurements by presenting misclassification rates as a function of energy.

The physics behind PSD relies on the fact that neutrons and gamma rays will deposit their energy in different ways in the scintillation material causing distinct pulse shapes. X-rays and gammas interact primarily

* Corresponding author.
E-mail address: amanda_lewis@berkeley.edu (A.M. Lewis).

https://doi.org/10.1016/j.nima.2018.05.024
Received 7 December 2017; Received in revised form 26 April 2018; Accepted 12 May 2018
Available online 22 May 2018
0168-9002/

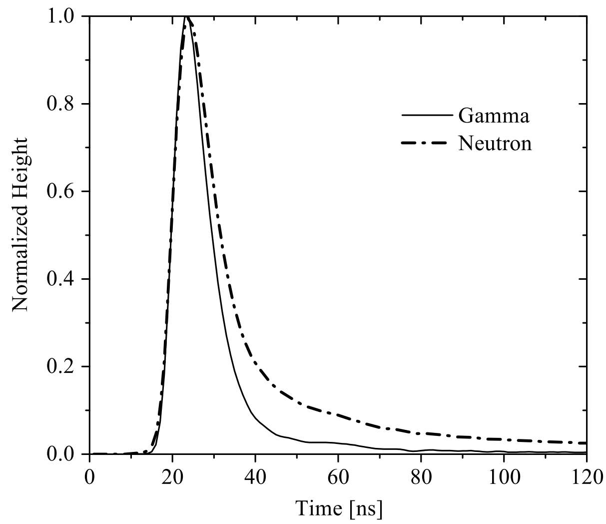

Fig. 1. Average normalized pulse shapes obtained from gammas interactions and from neutron interactions. It can be seen that the two shapes have very similar rise times, but disparate fall times, caused by the neutron exciting longer lived states. Unknown pulses were characterized based on channels 40 through 60 ns, as this was the area of largest difference between the two pulse shapes.

with the electrons in the scintillation material, and the majority of the signal is prompt fluorescence. Conversely, recoil protons produced by neutron interactions excite triplet states which are longer lived and slow the decay of the response pulse [7]. For this reason, with sufficient timing resolution, a pulse caused by a neutron interaction can be distinguished from a pulse caused by a gamma interaction. This method has been proven to be very successful at neutron energies above 500 keV where the amount of energy deposited in the scintillator is enough to have high signal-to-noise ratios [2]. Fig. 1 shows typical average pulse shapes for gamma and neutron interactions in an EJ-301 liquid scintillator which highlights the longer decay time for neutron pulses and the short decay time for gammas.

At lower energies, the pulse height is similarly lower and the electrical noise in the system begins to have a more significant effect, which can be seen in Figs. 2 and 3. In Fig. 2, two gamma pulses of differing heights are shown, and for each the noise from the electronics is of similar magnitude. When the pulses are normalized to unit height, shown in Fig. 3, the noise becomes much more significant in the shape of the smaller pulses. This increased noise level can cause gamma pulses to look more similar to the neutron pulses due to the noise causing the pulse to appear to have a longer decay time. In this work, the pulse shape classification (PSC) method previously developed at Rensselaer Polytechnic Institute (RPI) [8] is further developed to accurately characterize pulses in the low energy region where that noise is significant.

2. Experimental setup

The detector used for these measurements was a 12.7 cm diameter, 1.27 cm thick EJ-301 liquid scintillation detector coupled to a 12.7 cm diameter Electron Tubes 9823B series photomultiplier tube. The pulses were recorded using an Acqiris AP240 8-bit digitizer with GHz sampling rate (1 ns resolution). The detector thickness was chosen to minimize the gamma background while still providing sufficient neutron detection efficiency. This allowed the bias voltage to be set to 2200 V in order to amplify the low energy pulses.

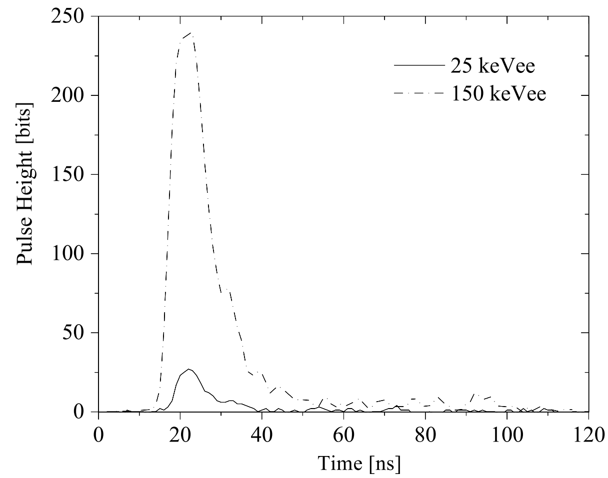

Fig. 2. Two gamma response pulses of differing pulse heights. Each channel represents one nanosecond. The electrical noise, which can be seen easily in between 60 and 120 ns, is on the same scale for both pulses.

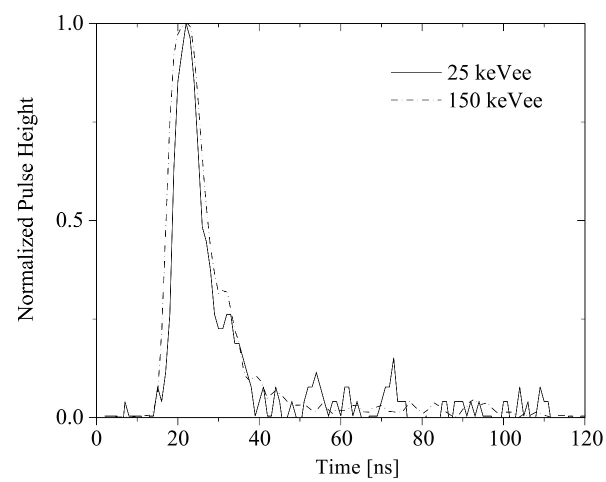

Fig. 3. The same two gamma response pulses of differing heights, normalized to the height of the peak channel. Each channel represents one nanosecond. The electrical noise for the smaller pulse is much larger relative to the pulse size and has a more significant effect on the shape of the pulse.

3. Method

3.1. Energy calibration

In order to determine the lowest measurable energy for the system, a correlation between the pulse integral and the incident gamma ray energy must be determined. Energy calibration was performed with two gamma sources, a 43.8 mCi ^{241}Am source, utilizing the 59.5 keV decay gamma, and a 3.53 μCi ^{137}Cs source, utilizing the 30.97 keV self florescence gamma. The correlation is presented in the equation in Fig. 4. This shows that the lowest detectable energy deposition is approximately 13 keVee.

3.2. Average pulse shape determination

The PSC method used in this work relies on determining average neutron and gamma pulses and doing a comparison to determine if an unknown pulse is more similar to the gamma or the neutron average shape. The determination of these average pulse shapes can be shown in the following sections.

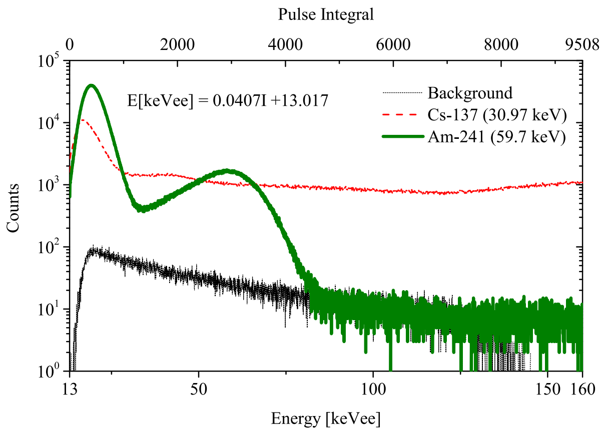

Fig. 4. Pulse integral spectrum obtained with EJ-301 detector at bias voltage of 2200 V. Two gamma sources, ^{241}Am and ^{137}Cs, were used to determine the energy-integral relation, shown on the plot, in which I is the pulse integral, and E is the corresponding deposited energy. This was done by calibrating to the 59.5 keV decay gamma from Am and the 30.97 keV self florescence line from ^{137}Cs.

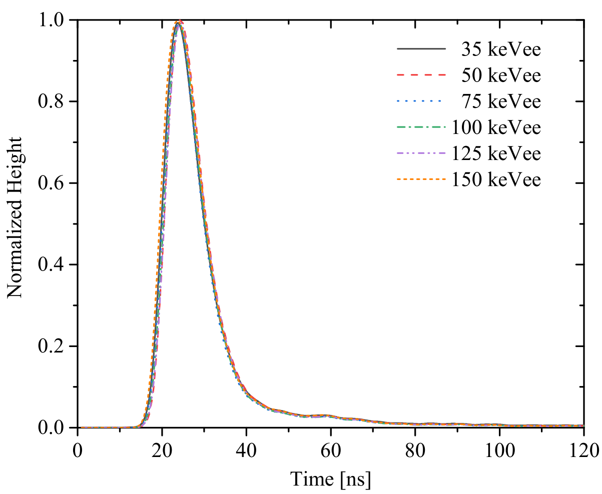

Fig. 5. Average normalized gamma pulse shapes in several energy deposition regions. It can be seen that the average pulse shape does not change significantly with energy deposition in the detector in this region.

In order to determine the average gamma pulse shape, one million gamma pulses from a ^{137}Cs source were used. These pulses were grouped corresponding to the energy deposited in the detector and subsequently peak aligned and normalized. These pulses were then averaged together to acquire average pulse shapes for each energy deposition region up to the maximum energy deposition of 160 keVee. Fig. 5 shows the height normalized average gamma pulse shapes for various energy depositions and highlights that the average gamma pulse shape is independent of the energy deposited in the detector. This indicates that one average gamma pulse shape could be used over the entire energy region of interest.

Average neutron pulses are harder to obtain as it is difficult to find a pure neutron source. Therefore, pulses were collected from a ^{252}Cf spontaneous fission source and a crude fall time analysis was performed to determine neutron from gamma events. The fall time of a pulse, defined here as the time between 10% and 87% of the full pulse integral, is a measure of the decay of the signal and so is representative of the interacting particle. A ^{252}Cf source with a rate of 8.76 neutrons/s was placed 30.5 cm away from the detector, behind two inches of lead to minimize the gamma flux on the detector. Fig. 6 presents the fall time vs. total integral scatter plot of these pulses, which shows a distribution of

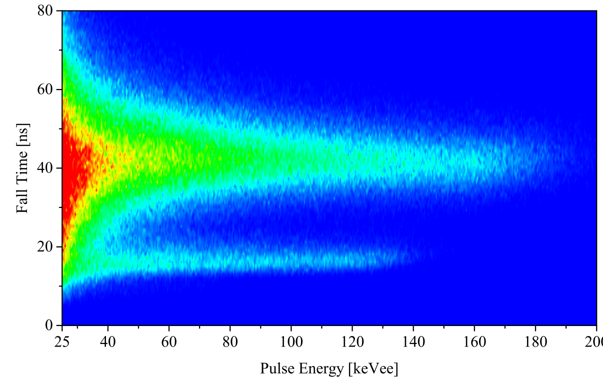

Fig. 6. Fall time-integral scatterplot for lead-shielded ^{252}Cf source. There is good separation between the gamma pulses and neutron pulses down to an integral of 35 keVee, at which point the two clusters overlap.

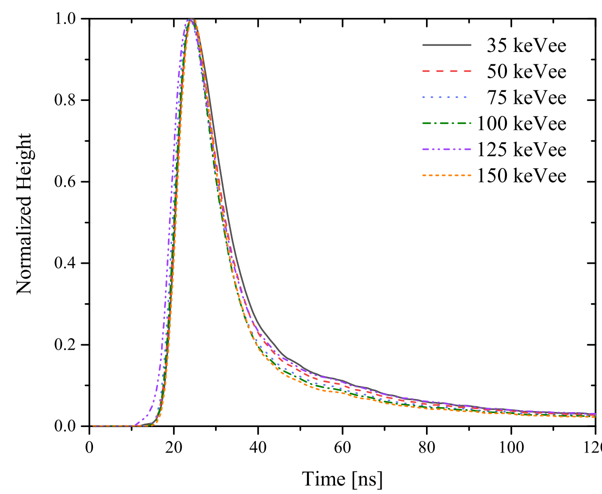

Fig. 7. Average normalized neutron pulse shapes for several energy deposition regions. It can be seen that the shape of the pulse does not change significantly with energy deposition in the detector in this region.

pulses with a fall time below 20 ns, consistent with gamma pulses, and a distribution of pulses with higher fall times, which are the neutrons. The average neutron shape was found by using pulses with an energy greater than 35 keVee and a fall time greater than 30 ns, as these were far from the overlap with the gamma distribution. These pulses were grouped corresponding to the energy deposited in the detector and subsequently peak aligned and normalized similar to the gamma pulses and the average pulse shape for neutrons of various energy deposition can be seen in Fig. 7. While the neutron distribution is wider than the gamma distribution, the neutron pulses still consistently decay more slowly than the gammas pulses and are different enough from the gamma shape that one average neutron pulse shape can be used over the entire energy region.

3.3. Pulse shape classification (PSC)

Unknown pulses were characterized by comparison to the average pulse shapes shown in Fig. 1 and determination of which of the two shapes the unknown pulse was most similar to. To do so, the squared residual value with respect to each average pulse was found between 40 and 60 ns, shown in Eqs. (1) and (2), as this is the region of largest difference between the two average pulse shapes. The unknown pulse was classified by the average shape that produced the lower of the two

Table 1
Classification of background subtracted gamma sources using the PSC method in the full energy deposition range from 35 keVee to 400 keVee.

Source	Gamma pulses	Neutron pulses
^{241}Am	305 423 (**99.5%**)	1403 (**0.5%**)
^{137}Cs	1 044 601 (**99.5%**)	5296 (**0.5%**)

R^2 values.

$$R_n^2 = \sum_{i=40\text{ ns}}^{60\text{ ns}} (P_i - P_i^n)^2 \tag{1}$$

$$R_\gamma^2 = \sum_{i=40\text{ ns}}^{60\text{ ns}} (P_i - P_i^\gamma)^2. \tag{2}$$

This classification was very accurate for pulses above 420 keVee (less than 0.1% of pulses were misclassified) but at the low end of the energy region there was an overlap between the gamma and neutron classification where pulses began to be misclassified. As the purpose of this detector and post-processing method is for use in neutron detection, the focus of this work is on the misclassification of gamma signals as neutrons, rather than misclassification of neutrons as gammas. An energy-dependent neutron detection efficiency, including the post-processing, would need to be measured before use in a measurement; misclassified neutrons would just reduce this efficiency. The gamma misclassification is a problem because the misclassified gamma signals would contribute to the measured neutron signal. For this reason, the magnitude of the gamma misclassification is studied here.

4. Quantification of gamma misclassification

In order to determine the extent to which gamma pulses were misclassified as neutrons, experiments were performed with gamma sources and this pulse shape classification method.

4.1. Gamma source characterization

Separate measurements were performed to measure a ^{137}Cs source, an ^{241}Am source and the room background rate. These measurements were processed using the PSC technique and the number of corresponding neutron and gamma pulses were obtained. The background counts were subtracted from the source counts in order to eliminate the natural neutron background contribution. Table 1 shows the number of pulses classified as neutrons and gammas for the background subtracted sources. The percentage of total pulses that were recorded as neutrons is referred to as the total gamma misclassification rate. The results of this characterization were grouped into energy deposition bins of 10 keVee, and are presented in Fig. 8. The percent misclassification is also compared to that of the analysis using just the fall time of the pulse. This comparison shows that for the lower energy bins, where improvement is most needed, the use of this method further increases the improvement in classification attained by using a thinner detector at a higher voltage.

The pulse shape characterization method misclassified only 2% of the gamma pulses between 35 keVee and 45 keVee, which were the smallest pulses and so had the most amplified noise. Additionally, over the entire energy range of interest only 0.5% of all gamma pulses were misclassified as neutrons. Therefore, this misclassification will only be an issue for measurements with very high fluxes of low energy background gammas.

5. Validation by neutron time-of-flight

A source of neutrons of known energy was created using the Gaerttner Linear Accelerator Facility at Rensselaer Polytechnic Institute [9,10]. A pulsed neutron beam from the LINAC interacted with a carbon sample placed 30.07 m away from the neutron source. Neutrons

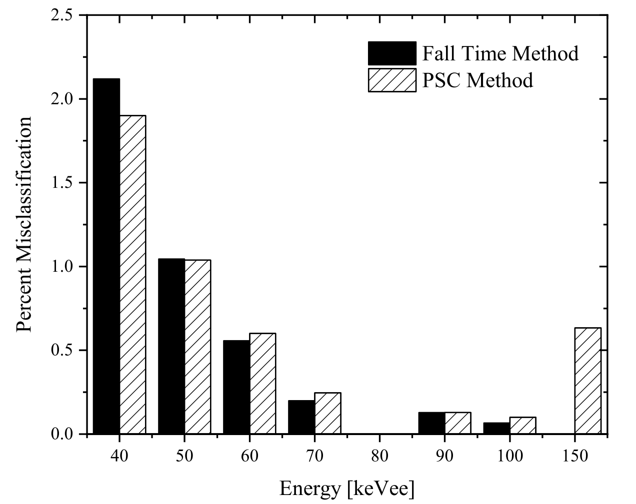

Fig. 8. Characterization of ^{137}Cs gamma source data using the pulse shape characterization method, with a maximum misclassification of 2% at the 35 keVee–45 keVee pulses bin. The misclassification rate drops significantly as the energy increases. This misclassification rate is compared to the classification with the fall time method, which shows that the PSC method is more accurate in the low energy bins.

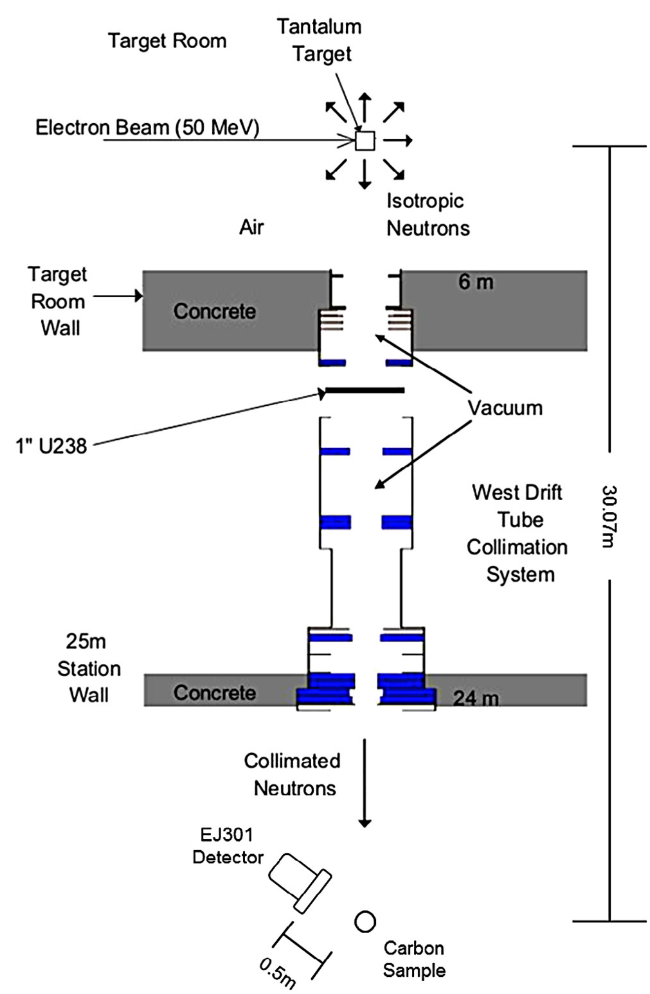

Fig. 9. Diagram of neutron beam experiment. The neutrons are produced at a tantalum target, then travel 30.07 m to the carbon scattering sample. Neutrons that are scattered by 153° will then travel 0.5 m to the detector.

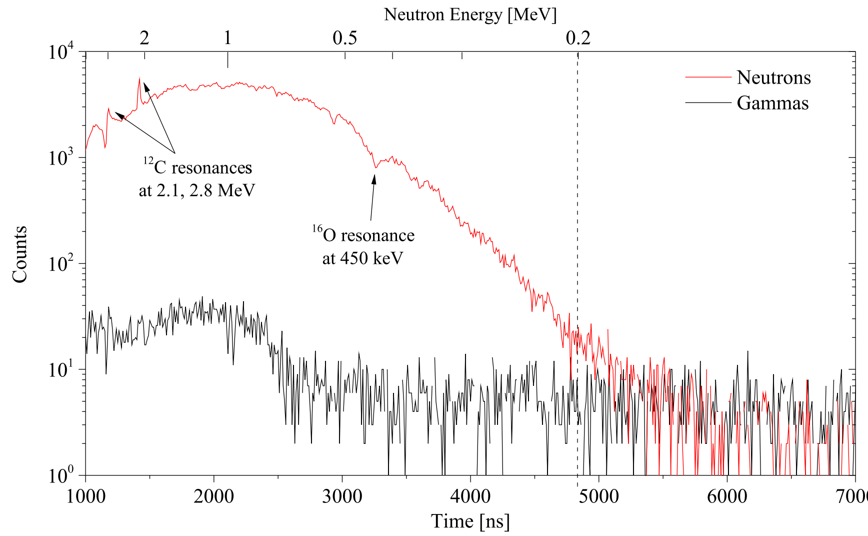

Fig. 10. TOF spectra of neutrons backscattered off of a carbon sample and gammas from inelastic scattering and background, based on the PSC method with GM correction. Resonance structure can be seen in the neutron spectrum, but not in the gamma spectrum, validating the time-of-flight conversion to energy, and showing that there is not a significant problem with misclassifying neutrons as gammas.

that scattered at an angle of 153° were detected by the EJ-301 detector that was placed 0.5 m from the carbon sample. The LINAC operated with a pulse width of 8 ns. This backscattering geometry was chosen to minimize the gamma background. The time of flight method was used to determine the energy of the neutrons, as shown in Eq. (3), in which L is the flight path of the neutrons, 30.57 m, t is the time the neutron was detected and γ is the time at which the neutrons were produced, relative to the DAQ trigger. See Fig. 9 for the locations of the carbon scattering sample and detector in relation to the neutron beam.

$$E\ [\text{eV}] = \left(\frac{72.3L}{t\ [\mu\text{s}] - \gamma}\right)^2. \tag{3}$$

5.1. Low energy neutron characterization

The PSC method was used to characterize neutrons between 1000 and 6000 ns, as shown in Fig. 10, which corresponds to the energy range of 5 MeV to 135 keV. The large carbon resonances at 2.1 MeV and 2.8 MeV can be seen in the neutron spectrum, validating the conversion from time-of-flight to energy. The drop in the spectrum at 3400 ns corresponds to the oxygen resonance at 0.45 MeV, as there was some air in the path of the neutrons. This resonance was too low in energy to be seen by the previous EJ-301 work [11] but can clearly be seen here. The gammas seen in Fig. 10 are from the background, and so the time of detection does not correspond to a specific gamma energy. For this reason, resonance structure in the gammas would indicate that there was a significant problem with misclassifying neutrons as gammas. It can be seen that past 2500 ns there is no structure in the gammas, indicating that this is not a problem. Before 2500 ns there is an increase in the number of detected gammas, which is a result of the higher background in the room because of the accelerator and the gammas created in the target.

6. Conclusions

This work extends the range of pulse shape discrimination for liquid scintillators to much lower energies allowing for measurements in this range to be performed with much higher efficiency detectors, compared to current measurements using ^{6}Li. Accurate detection and classification of neutron and gamma pulses has been demonstrated using a 1.27 cm thick EJ-301 detector operated at a high bias voltage down to a neutron energy of 200 keV and has been validated by measuring carbon scattering response from neutron time-of-flight measurements. This classification has been achieved with the low gamma misclassification rate of 0.5% from the energy range of 35 keVee to 400 keVee, and 2% in the lowest energy range from 35 keVee to 45 keVee.

Acknowledgments

The authors express their appreciation to the LINAC staff for their expertise and diligent work. The authors also thank the Stewardship Science Academic Alliance for their funding of this research, Grant numbers: DE-FG5209NA29453, DE-NA0001814.

References

[1] V.N. Kononov, E.D. Poletaev, M.V. Bohovko, L.E. Kazakov, V.M. Timohov, P.P. Dyachenko, L.S. Kutsaeva, E.A. Seregina, A. Lajtai, J. Kecskeméti, Neutron detection efficiency of a thick lithium glass detector, Nucl. Instrum. Methods Phys. Res. A 234 (2) (1985) 361–366. http://dx.doi.org/10.1016/0168-9002(85)90929-5.
[2] F.J. Saglime, Y. Danon, R.C. Block, M.J. Rapp, R.M. Bahran, G. Leinweber, D.P. Barry, N.J. Drindak, A system for differential neutron scattering experiments in the energy range from 0.5 to 20 MeV, Nucl. Instrum. Methods Phys. Res. A 620 (2–3) (2010) 401–409. http://dx.doi.org/10.1016/j.nima.2010.04.051.
[3] R.F. Lang, D. Masson, J. Pienaar, S. Röttger, Improved pulse shape discrimination in EJ-301 liquid scintillators, Nucl. Instrum. Methods Phys. Res. A 856 (2017) 26–31. https://doi.org/10.1016/j.nima.2017.02.090. http://www.sciencedirect.com/science/article/pii/S0168900217303133.
[4] W. Bo, X.-Y. Zhang, C. Liang, G. Hong-Lin, M. Fei, H.-B. Zhang, J. Yong-Qin, Z. Yan-Bin, L. Yan-Yan, X. Xiao-Wei, Study of digital pulse shape discrimination method for $n-\gamma$ separation of EJ-301 liquid scintillation detector, Chin. Phys. C 37 (1) (2013) arXiv:1502.01807v1. https://arxiv.org/pdf/1502.01807.pdf.
[5] P. Kendall, K. Duroe, P. Arthur, M. Ellis, M.C. Owen, R.S. Woolf, E.A. Wulf, A.L. Hutcheson, B.F. Phlips, Comparative study of the pulse shape discrimination (PSD) performance of fast neutron detectors, in: 2014 IEEE Nuclear Science Symposium and Medical Imaging Conference, NSS/MIC, 2014, pp. 1–6.
[6] S.D. Ambers, M. Flaska, S.A. Pozzi, A hybrid pulse shape discrimination technique with enhanced performance at neutron energies below 500 keV, Nucl. Instrum. Methods Phys. Res. A 638 (1) (2011) 116–121. http://dx.doi.org/10.1016/j.nima.2011.01.119.
[7] G. Knoll, Radiation Detection and Measurement, third ed., John Wiley and Sons Inc., 2000.
[8] A. Daskalakis, Measurement of Elastic and Inelastic Neutron Scattering in the Energy Range from 0.5 to 20 MeV (Ph.D. thesis), Rensselaer Polytechnic Institute, Troy, NY, 2016.
[9] F.J. Saglime, High Energy Neutron Differential Scattering Measurements for Beryllium and Molybdenum (Ph.D. thesis), Rensselaer Polytechnic Institute, Troy, NY, 2009.
[10] M.E. Overberg, B.E. Moretti, R.E. Slovacek, R.C. Block, Photoneutron target development for the RPI linear accelerator, Nucl. Instrum. Methods Phys. Res. A 438 (2–3) (1999) 253–264. http://dx.doi.org/10.1016/S0168-9002(99)00878-5.
[11] A.M. Daskalakis, R.M. Bahran, E.J. Blain, B.J. McDermott, S. Piela, Y. Danon, D.P. Barry, G. Leinweber, R.C. Block, M.J. Rapp, R. Capote, A. Trkov, Quasi-differential neutron scattering from 238U from 0.5 to 20 MeV, Ann. Nucl. Energy 73 (2014) 455–464. http://dx.doi.org/10.1016/j.anucene.2014.07.023.